

A Heuristic-Sliding-Window-based RRT Path Planning for Endovascular Catheterization

Zhen Li^{1,2}, Alice Segato¹, Alberto Favaro¹, Jenny Dankelman² and Elena De Momi¹

¹ *Department of Electronics, Information and Bioengineering, Politecnico di Milano, Milan, Italy*

² *Department of Biomechanical Engineering, Delft University of Technology, Delft, The Netherlands*

{zhen.li, alice.segato, alberto.favaro, elena.demomi}@polimi.it

{Z.Li-13, j.dankelman}@tudelft.nl

Abstract—Catheter interventions are often used in endovascular procedures to obviate complicated open surgical interventions. One of the major challenges relates to moving the catheter toward the required location with safety and accuracy. Due to the unpredictable tissue deformation associated with device insertion and the uncertainties of intra-operative sensing, a fast and robust path planning algorithm would be advantageous. Most of current methods are pre-operative planning, ignoring time costs. This paper aims at proposing a faster and robust path planning algorithm based on heuristics information. In this paper, a novel Heuristic-Sliding-Window-based Rapidly-exploring Random Trees (HSW-RRT) path planning algorithm is proposed for endovascular catheterization. This method keeps the catheter away from vascular edges in light of safety concerns by sampling along the centerline. Simulation results show the feasibility of this path planning method in 2D scenarios. Path solutions can be generated with similar performance and less time effort than RRT*.

Keywords—Path Planning, Flexible Catheter, Autonomous Endovascular Intervention

I. INTRODUCTION

In Peripheral Artery Disease (PAD), arteries become narrowed or blocked, usually as a result of atherosclerosis or plaque. Total occlusion of the superficial femoral artery is present in up to 50% of patients showing symptoms of PAD [1]. For treatment of it, the standard approach has been to access the contralateral common femoral artery.

Catheters are one of the most versatile and essential instruments used in endovascular interventions. For example, it can be used to cannulate the femoral arteries by pushing the plaque aside and placing a stent nearby to restore and maintain the blood circulation as shown in Fig. 1. One of the major challenges relates to moving the catheter toward the required location with accuracy and safety.

Due to the narrow, tortuous, slender and unstructured blood vessels, the path planning for autonomous endovascular interventions becomes complicated. Many of the path planning for endovascular interventions are graph-based methods, sampling tree nodes along the vascular centerlines, as in [3]–[12]. The isobars under the steady fluid condition are applied instead of centerlines in [13]. The Dijkstra, A*, breadth-first searching and other standard searching algorithms are able to find the optimal path, while the nonholonomic constraints are ignored and they are time consuming. Moreover, the application scenario

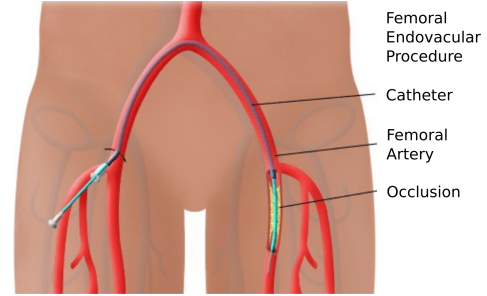


Fig. 1: Femoral endovascular procedure [2]

is limited to path planning in a static environment, ignoring the deformation of soft tissues during the clinical procedures. Learning based methods are also applied in endovascular navigation as in [14]–[18], while the data collection process for a specific application scenario is time consuming and the black box effect can not be ignored, which brings potential risks.

Sampling-based methods are developed well in mobile robots, and there is a lot of room for improvement on autonomous endovascular interventions. Probabilistic Roadmaps (PRM), Rapidly-exploring Random Trees (RRT) [19], [20], Fast Marching Trees (FMT) [21], Adaptive Fractal Trees (AFT) and their derivatives have attracted increasing attention recently. Nevertheless, in those papers they are pre-operative planning, ignoring the dynamic environments and real-time requirements. Due to the unpredictable tissue deformation associated with device insertion and the uncertainties of intra-operative sensing, a real-time path planning algorithm with high update frequency would be advantageous.

In this paper, a fast and robust path planning algorithm based on Rapidly-exploring Random Trees with a Heuristic Sliding Window is proposed for catheter interventions in endovascular procedures. (i) This method tries to keep the catheter away from vessel edges in light of safety concerns by sampling along the centerline. (ii) Instead of sampling in the overall search space, this method uses heuristics to improve the sampling efficiency. (iii) Considering the uncertainties of flexible robot model and deformations of soft tissues during the procedures, the proposed path planning method allows faster path re-planning intra-operatively than RRT*. (iv) Sim-

ulation results in 2D scenarios show the feasibility of this path planning method. The path solutions are compared with that of RRT and RRT*, evaluating by time cost, path length and maximal curvature.

In this paper, the methodology is introduced in Sec. II, and the simulation results using different methods are discussed in Sec. III. Conclusions and future work are presented in Sec. IV.

II. METHODS

A. Search space

The original image in Fig. 2 is a 2D 294×220 digital subtraction angiography image from [22] with a virtual occlusion on the left side. It is segmented firstly via watershed algorithm and centerline is extracted via medial axis skeletonization.

Keeping away from vascular edges should be considered in light of safety concerns. If the search space is considered as the same as the collision free space inside blood vessels, the edge segment (red line in Fig. 3c) between 2 vertices sometimes is close to the vascular edges (orange contour). In that case, the catheter deployment can be dangerous as it can damage the deformable vessel tissue.

The image erosion and dilation are efficient and mature ways to shrink the free space, and they perform image convolution operations. Therefore, the path will locates in a search space which is smaller than the original collision free space, respectively the blue and orange zones in Fig. 2.

B. HSW-RRT

The Heuristic-Sliding-Window-based RRT (HSW-RRT) is a sampling-based path planning algorithm. The tree is constructed incrementally from samples drawn randomly from the search space. Instead of randomly sampling in overall search space, this method uses a heuristic sliding window to improve the sampling efficiency.

The heuristic sliding window is defined as a strip-shaped area, which is expanded from the centerline with an adaptive width as shown in Fig. 3a. In order to keep away from the vascular edges as far as possible, the window in this paper is limited to the centerline segment without strip width (i.e. the purple curve in Fig. 3a) and the window length is a user-defined parameter. This window is centered at the tree vertex (i.e. the blue point in Fig. 3a), which has the minimal cost function value as (1).

The function $cost_to_come$ returns the cumulative path length from the tree root to current node x . $cost_to_go$ indicates the cost to the goal location from current node x , and it can be represented by the Euclidean distance from x to the goal location.

$$\begin{aligned} f(x) &= cost_to_come(root, x) + h(x) \\ h(x) &= cost_to_go(x, goal) \end{aligned} \quad (1)$$

Even if the samples are generated on the centerline, it does not mean that the connected edge between vertices strictly locates on the centerline as shown in Fig. 3b. In order to avoid getting stuck in a local minimum (i.e. keeping sampling locally around the vertex with minimal cost without exploring other

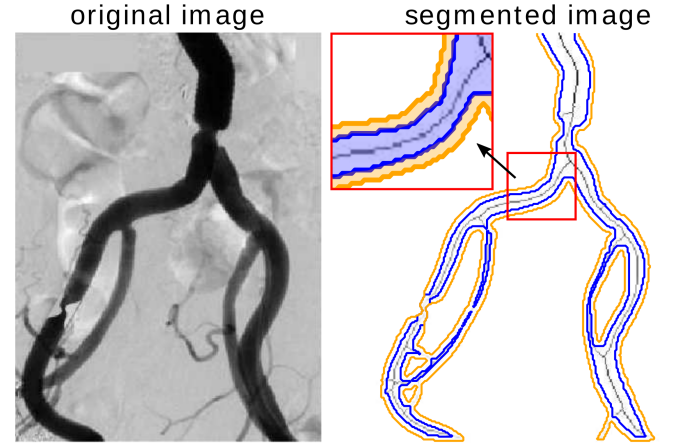


Fig. 2: Image segmentation and centerline extraction. The contour of segmented vessel is presented with orange line and the centerline is shown with greys heat map. The darker is the centerline color, the longer is the distance from vessel edges. The search space is defined as the zone within the blue contour.

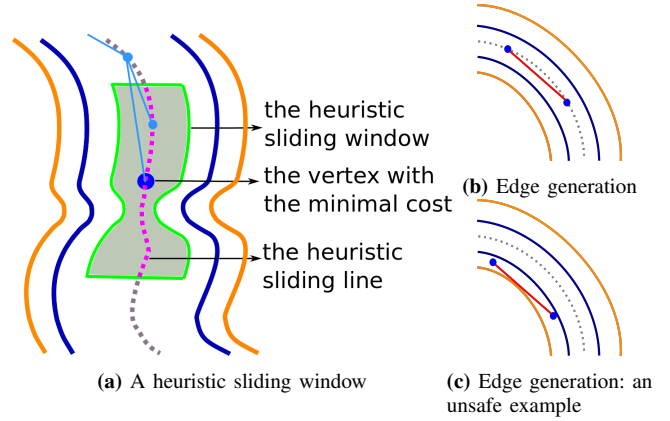


Fig. 3: HSW-RRT tree construction

possibilities), the sample should also be randomly generated in the overall centerline strip at a certain rate. For more details, see the pseudocode in Algorithm 1.

C. Path smoothing

The path solution obtained from HSW-RRT is a list of setpoints. The non-differentiable connections between line segments will exceed the robot manipulability. Path smoothing is required to meet robot's kinematics, i.e. the curvature of path should be bounded.

B-Spline is a spline function that has local support with respect to a given degree, smoothness, and domain partition. Given a knot sequence $t_0, \dots, t_i, \dots, t_m$, $m+1$ B-splines with degree n can be defined by construction by means of the Cox-de Boor recursion formula as in (2).

$$\begin{aligned} b_{i,0}(x) &= \begin{cases} 1 & t_i \leq x < t_{i+1} \\ 0 & \text{otherwise} \end{cases} \\ b_{i,n}(x) &= \frac{x - t_i}{t_{i+n} - t_i} b_{i,n-1}(x) + \frac{t_{i+n+1} - x}{t_{i+n+1} - t_{i+1}} b_{i+1,n-1}(x) \end{aligned} \quad (2)$$

The curvature at point (x, y) can be defined as (3). The maximal curvature of final path is evaluated as the smoothness

Algorithm 1 HSW-RRT**Input:** search space X , initial and goal point x_{init} , x_{goal} **Output:** path solution**Parameter:** maximum edge length q , number of child vertices k , maximum number of samples n_{max} , resolution of points when checking collision, probability of checking solution, probability of sampling in overall free space p

```

1: procedure HSW-RRT PATH SEARCHING
2:   initialization(inputs and parameters)
3:   add_vertex( $x_{init}$ )
4:   add_edge( $x_{init}$ )
5:   while true do
6:     for  $i$  in  $q$  do
7:       for  $j$  in  $(1 : k)$  do
8:         if random()  $< p$  then
9:            $x_{rand} \leftarrow \text{random\_centerline}()$ 
10:        else
11:           $x_{rand} \leftarrow \text{random\_hsw}(f_x)$ 
12:           $x_{near} \leftarrow \text{nearest\_vertex}(x_{rand})$ 
13:           $x_{new} \leftarrow \text{new\_vertex}(x_{rand}, x_{near}, i)$ 
14:          add_vertex( $x_{new}$ )
15:           $L_x, L_c, f_x \leftarrow \text{get\_nearby\_vertices}(x_{new})$ 
16:           $\triangleright$  get the list of nearby vertices  $L_x$  with their cost-to-come
17:           $L_c$  and the node with minimal cost function value  $f_x$ 
18:          add_vertex( $x_{new}$ )
19:          add_shortest_edge( $L_x, x_{new}$ )
20:          rewire_tree( $L_x, x_{new}$ )
21:           $sol \leftarrow \text{check\_solution}()$ 
22:          if  $sol$  is true then return path
23:           $\triangleright$  exit loop when finding a path or reaching  $n_{max}$ 

```

in order to inspect the catheter nonholonomic constraints as index of performance.

$$\text{curvature}(x, y) = \frac{|\dot{x}\ddot{y} - \dot{y}\ddot{x}|}{(\dot{x}^2 + \dot{y}^2)^{\frac{3}{2}}} \quad (3)$$

III. RESULTS

The simulation is carried out in the PyCharm platform on a computer with Ubuntu system. This computer is equipped with an Intel (R) Core (TM) i5-8250U CPU @ 1.60 GHz 1.80 GHz processor and 8 GB RAM.

The simulation results of path planning via RRT, RRT* and HSW-RRT are shown in Fig. 4-7. The proposed method is also validated in another case as Fig. 7, which is a part of the vascular tree in the leg from [23]. The initial and goal location are the black and purple points, respectively. Blue line represents the tree expansion during the path searching procedure. Green line depicts the generated path after searching. And red line shows the final solution after path smoothing.

The performance evaluation of the proposed method is summarized in TABLE I, compared with traditional RRT series methods. The time cost, the path length, and the path maximal curvature are evaluated from 10 sets of start and goal states. The time cost is determined not only by the path planning

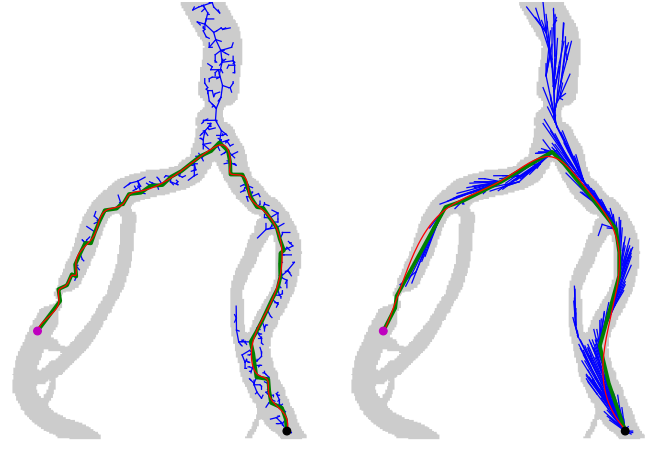


Fig. 4: The simulation result of RRT path planning

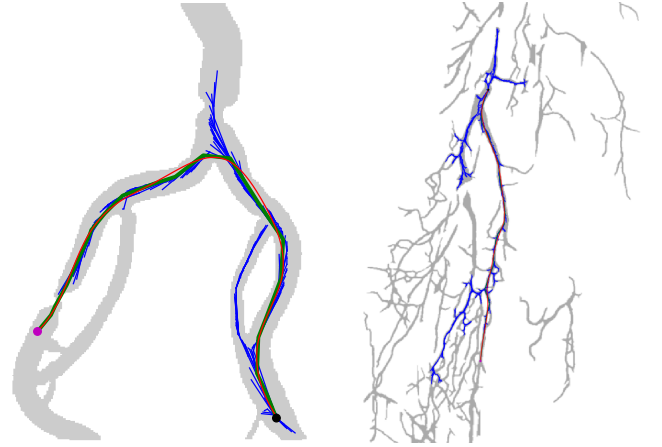


Fig. 5: The simulation result of RRT* path planning

Fig. 6: The simulation result of HSW-RRT path planning: case 1

Fig. 7: The simulation result of HSW-RRT path planning: case 2 (from [23])

method, but also by the entry and the target points, i.e. the time cost varies upon different scenarios. The HSW-RRT generates a path solution with similar length and smoothness as RRT*, and takes less time effort than it. Even if HSW-RRT takes longer time than RRT, it's still worthwhile, considering the quality of path. If the femoral endovascular procedure takes from 45s to 25s [24], and the maximum bending angle is around $77^\circ/cm$ (i.e. 0.086 rad/px in Fig. 6), the path planning algorithm is reasonable. The catheter in [25] is designed with a maximum bending angle $61^\circ/cm$, which means the path can be infeasible if the nonholonomic constraints are ignored during path planning.

TABLE I: The performance comparison.

Method	Time (ms)	Length of Path (px)	Maximal Curvature (rad/px)
RRT	300.2 ± 100.1	420.1 ± 22.1	0.902 ± 0.675
RRT*	4018.4 ± 1598.1	374.7 ± 6.8	0.070 ± 0.026
HSW-RRT	1598.2 ± 276.2	373.1 ± 9.9	0.086 ± 0.050

Note: 10 sets of start and goal locations are tested, which is $(283 \pm 4, 183 \pm 3)$ and $(218 \pm 3, 22 \pm 3)$, respectively.

IV. CONCLUSION

In this paper, a novel HSW-RRT method is proposed for endovascular catheterization. Instead of randomly sampling in the overall search space, this method uses a heuristic sliding window to improve the sampling efficiency. In order to avoid getting stuck in a local minimum, the sample should also be randomly generated in the overall centerline strip at a certain rate. Simulation results show the feasibility of this path planning method in 2D scenarios and the path solution can be generated around 1.6s for femoral endovascular catheterization. The HSW-RRT generates a path solution with similar length and smoothness as RRT*, and takes less time effort than it. Even though HSW-RRT takes longer time than RRT, it's still worthwhile, considering its reliability.

Later on, (i) the nonholonomic constraints should be expressed as bounded curvature, and controlled quantitatively via path smoothing or edge construction; (ii) the path planning will be implemented in 3D scenarios and the computational velocity will be improved; (iii) a re-planning algorithm based on initial path should be proposed when the deformation of environments is detected, taking the advantage of pre-operative path; (iv) if the full 3D model can not be reconstructed in real-time, vision servoing based control can be used for the intra-operative navigation of catheter by using 2D images, which will be investigated and implemented in the future.

ACKNOWLEDGEMENT

This project has received funding from the European Union's Horizon 2020 research and innovation programme under the Marie Skłodowska-Curie grant agreement No 813782.

This work is not being and has not been submitted for publication or presentation elsewhere.

REFERENCES

- [1] L. L. Nadal, J. Cynamon, E. C. Lipsitz, and A. Bolia, "Subintimal angioplasty for chronic arterial occlusions," *Techniques in vascular and interventional radiology*, vol. 7, no. 1, pp. 16–22, 2004.
- [2] AICD, "Cardiology patient education." [Online]. Available: www.aicdheart.com/patient_education/heart_HTML_scaleable/heart/fempop.htm
- [3] B. Geiger, A. P. Kiraly, D. P. Naidich, and C. L. Novak, "Virtual bronchoscopy of peripheral nodules using arteries as surrogate pathways," in *Medical Imaging 2005: Physiology, Function, and Structure from Medical Images*, A. A. Amini and A. Manduca, Eds. SPIE, Apr. 2005.
- [4] W. Sabra, M. Khouzam, A. Chanu, and S. Martel, "Use of 3d potential field and an enhanced breadth-first search algorithms for the path planning of microdevices propelled in the cardiovascular system," in *2005 IEEE Engineering in Medicine and Biology 27th Annual Conference*. IEEE, 2006, pp. 3916–3920.
- [5] S. Schafer, V. Singh, K. R. Hoffmann, P. B. Noël, and J. Xu, "Planning image-guided endovascular interventions: guidewire simulation using shortest path algorithms," in *Medical Imaging 2007: Visualization and Image-Guided Procedures*, K. R. Cleary and M. I. Miga, Eds. SPIE, Mar. 2007.
- [6] K. Ratnayaka, T. Rogers, W. H. Schenke, J. R. Mazal, M. Y. Chen, M. Sonmez, M. S. Hansen, O. Kocaturk, A. Z. Faranesh, and R. J. Lederman, "Magnetic resonance imaging-guided transcatheter cavopulmonary shunt," *JACC: Cardiovascular Interventions*, vol. 9, no. 9, pp. 959–970, May 2016.
- [7] C. Sánchez, M. Diez-Ferrer, J. Bernal, F. J. Sánchez, A. Rosell, and D. Gil, "Navigation path retrieval from videobronchoscopy using bronchial branches," in *Clinical Image-Based Procedures. Translational Research in Medical Imaging*. Springer International Publishing, 2016, pp. 62–70.
- [8] S. Martel, J.-B. Mathieu, O. Felfoul, A. Chanu, E. Aboussouan, S. Tamaz, P. Poupponneau, L. Yahia, G. Beaudoin, G. Soulez *et al.*, "Medical and technical protocol for automatic navigation of a wireless device in the carotid artery of a living swine using a standard clinical mri system," in *International Conference on Medical Image Computing and Computer-Assisted Intervention*. Springer, 2007, pp. 144–152.
- [9] Y. Chang, X. Wang, Z. An, and H. Wang, "Robotic path planning using a* algorithm for automatic navigation in magnetic resonance angiography," in *2018 40th Annual International Conference of the IEEE Engineering in Medicine and Biology Society (EMBC)*. IEEE, 2018, pp. 734–737.
- [10] Y. Xiao, W. Tan, Q. Zhou, and Y. Ji, "Pulmonary vascular segmentation algorithm based on fractional differential enhancement," in *International Conference on Mechatronics and Intelligent Robotics*. Springer, 2018, pp. 1262–1274.
- [11] F. Yang, Y. Dai, J. Zhang, H. Sun, L. Cui, X. Yin, X. Gao, and L. Li, "Path planning of flexible ureteroscope based on ct image," in *2019 Chinese Control Conference (CCC)*. IEEE, 2019, pp. 4667–4672.
- [12] K. Meng, Y. Jia, H. Yang, F. Niu, Y. Wang, and D. Sun, "Motion planning and robust control for the endovascular navigation of a microrobot," *IEEE Transactions on Industrial Informatics*, 2019.
- [13] D. Huang, P. Tang, Y. Wang, L. Hejuan, W. Tang, and Y. Ding, "Computer-assisted path planning for minimally invasive vascular surgery," *Chinese Journal of Electronics*, vol. 27, no. 6, pp. 1241–1249, 2018.
- [14] C. Tercero, S. Ikeda, T. Fukuda, F. Arai, M. Negoro, and I. Takahashi, "Catheter insertion reference trajectory construction method using photoelastic stress analysis for quantification of respect for tissue during endovascular surgery simulation," *International Journal of Optomechatronics*, vol. 5, no. 4, pp. 322–339, Oct. 2011.
- [15] H. Rafii-Tari, J. Liu, S.-L. Lee, C. Bicknell, and G.-Z. Yang, "Learning-based modeling of endovascular navigation for collaborative robotic catheterization," in *Advanced Information Systems Engineering*. Springer Berlin Heidelberg, 2013, pp. 369–377.
- [16] W. Chi, J. Liu, M. E. M. K. Abdelaziz, G. Dagnino, C. Riga, C. Bicknell, and G.-Z. Yang, "Trajectory optimization of robot-assisted endovascular catheterization with reinforcement learning," in *2018 IEEE/RSJ International Conference on Intelligent Robots and Systems (IROS)*. IEEE, Oct. 2018.
- [17] W. Chi, J. Liu, H. Rafii-Tari, C. Riga, C. Bicknell, and G.-Z. Yang, "Learning-based endovascular navigation through the use of non-rigid registration for collaborative robotic catheterization," *International Journal of Computer Assisted Radiology and Surgery*, vol. 13, no. 6, pp. 855–864, Apr. 2018.
- [18] X. Wang, Z. An, Y. Zhou, H. Wang, and Y. Chang, "Automating robot motion planning for magnetic resonance navigation using q-learning," in *2018 IEEE International Conference on Cyborg and Bionic Systems (CBS)*. IEEE, 2018, pp. 304–307.
- [19] L. G. Torres, R. J. Webster, and R. Alterovitz, "Task-oriented design of concentric tube robots using mechanics-based models," in *2012 IEEE/RSJ International Conference on Intelligent Robots and Systems*. IEEE, 2012, pp. 4449–4455.
- [20] C. Bergeles and P. E. Dupont, "Planning stable paths for concentric tube robots," in *2013 IEEE/RSJ International Conference on Intelligent Robots and Systems*. IEEE, 2013, pp. 3077–3082.
- [21] K. Belharet, D. Folio, and A. Ferreira, "Simulation and planning of a magnetically actuated microrobot navigating in the arteries," *IEEE Transactions on Biomedical Engineering*, vol. 60, no. 4, pp. 994–1001, 2012.
- [22] Y. Yokoi, "Basics of angiography for peripheral artery disease," *Angiography and Endovascular Therapy for Peripheral Artery Disease*, p. 1, 2017.
- [23] P. Bruno, P. Zaffino, S. Scaramuzzino, S. De Rosa, C. Indolfi, F. Calimeri, and M. F. Spadea, "Using cnns for designing and implementing an automatic vascular segmentation method of biomedical images," in *International Conference of the Italian Association for Artificial Intelligence*. Springer, 2018, pp. 60–70.
- [24] H. Clogenson, "Mri-compatible endovascular instruments: Improved maneuverability during navigation," 2014.
- [25] A. Ali, A. Sakes, E. A. Arkenbout, P. Henselmans, R. van Starckenburg, T. Szili-Torok, and P. Breedveld, "Catheter steering in interventional cardiology: Mechanical analysis and novel solution," *Proceedings of the Institution of Mechanical Engineers, Part H: Journal of Engineering in Medicine*, vol. 233, no. 12, pp. 1207–1218, 2019.